Rydberg dressing of a one-dimensional Bose-Einstein condensate

Marcin Płodzień,[1] Graham Lochead,[2] Julius de Hond,[2] N. J. van Druten,[2] and Servaas Kokkelmans[1]

[1]*Eindhoven University of Technology, P.O. Box 513, 5600 MB Eindhoven, The Netherlands*
[2]*Van der Waals-Zeeman Institute, University of Amsterdam, Science Park 904, 1098 XH Amsterdam, The Netherlands*

We study the influence of Rydberg-dressed interactions in a one-dimensional (1D) Bose-Einstein condensate (BEC). We show that a 1D geometry offers several advantages over a three-dimensional geometry for observing BEC Rydberg dressing. The effects of dressing are studied by investigating collective BEC dynamics after a rapid switch-off of the Rydberg dressing interaction. The results can be interpreted as an effective modification of the *s*-wave scattering length. We include this modification in an analytical model for the 1D BEC and compare it to numerical calculations of Rydberg dressing under realistic experimental conditions.

Ultracold quantum gas experiments allow for an extremely precise control of interatomic interactions. Strong interactions at the atomic level enable in principle the creation of strongly correlated many-body systems, where the tunability gives them an important advantage over their solid-state equivalents. The short-range interactions between ground-state atoms can be controlled by Feshbach resonances, which resulted, e.g., in the demonstration of the BCS–Bose-Einstein condensate (BEC) type superfluid crossover. However, while the interactions can be made very strong by going to the unitarity regime, it is still under debate whether this quantum gas can be considered as a strongly correlated system. Strong correlations will be evident when the interaction is both strong and long range, i.e., the range of the interaction exceeds the average interparticle separation. Rydberg atoms take a central role in the broad spectrum of systems that can be categorized from short range to long range, since Rydberg atoms can be classified as intermediate range. Their mutual interaction is generally of van der Waals nature, which is neither long range or short range: the van der Waals coefficient $C_6 \sim n^{11}$ scales rapidly with the principal quantum number n, allowing for a range larger than the interparticle separation.

Rydberg atoms in the context of ultracold atomic gases [1–12] open up a whole new direction of strongly correlated many-body physics with a focus on quantum computation and quantum simulations [13–19]. Most of the applications have their origin in the ability to manipulate these Rydberg atoms coherently on time scales below their radiative lifetime. When the atoms are cold enough, they remain spatially frozen at those time scales. Off-resonant coupling to Rydberg states, referred to as Rydberg dressing [10–12], allows experimentalists to achieve time scales longer than those required to stay in the frozen gas limit. These time scales enable BEC dynamics with long-range interactions, which are predicted to give rise to novel exotic many-body physics such as supersolidity [20–26].

Rydberg dressing of individual atoms trapped in optical tweezers [27] and in optical lattices [28] has been observed experimentally. Furthermore, modification of electromagnetically induced transparency (EIT) via resonant Rydberg dressing has also been observed [29]. However, observation of Rydberg dressing of a regular BEC has proven elusive so far. Rydberg dressing of a BEC in three dimensions (3D) has been theoretically studied [12,30–32] where at relatively low density the influence of dressing could be interpreted as a

modification of the *s*-wave scattering length. Rydberg dressing was also studied in one-dimensional geometry in the context of Rydberg impurities [33].

In Ref. [31], the authors conclude that experimental observation of a dressed BEC in 3D is very difficult due to a strong reduction in the amount of Rydberg atoms in the BEC caused by the Rydberg blockade mechanism. The characteristic density at which the blockade becomes dominant is very low, compared to typical BEC conditions in 3D, and even at densities below this characteristic value the dressing interaction is already strongly suppressed. Moreover, the interpretation as an effective modification of the scattering length is not obvious under these conditions.

Here, we consider a one-dimensional (1D) geometry and derive results for Rydberg dressing of 1D BECs. We show that these lead to much more favorable conditions for the observation of BEC dressing and that a sudden switch-off of the dressing interaction (via a switch-off of the dressing laser) results in collective BEC dynamics, which allows an interpretation in terms of an effective change of the *s*-wave scattering length. We show that the BEC breathing mode is a tenable experimental signature to observe BEC Rydberg dressing under realistic conditions, e.g., those typical for a 1D BEC trapped on an atom chip [34–36].

The advantages of the 1D geometry are twofold. First, it becomes much easier to work at densities *below* the characteristic blockade density. Second, the suppression of the Rydberg-dressed interactions by the blockade mechanism that is present even at low densities in 3D is much less severe in 1D. Both of these are evident in Fig. 1, which shows the behavior of the relevant energy functional for realistic experimental parameters (see below for details).

Before discussing the differences between 1D and 3D for Rydberg dressing of a BEC, it is useful to first quantitatively introduce the Rydberg-dressed two-body interaction [10–12]. For the purpose of this paper we limit ourselves to isotropic Rydberg dressing, by (two-photon) off-resonant coupling the electronic ground state of the atom to a Rydberg *S* state with the principal quantum number n. The key parameters are now the dressing parameter $\beta = \Omega/2|\Delta|$ and the blockade radius $R_B = (C_6/2\hbar\sqrt{\Delta^2 + \Omega^2})^{1/6} \approx (C_6/2\hbar|\Delta|)^{1/6}$, where Ω is the two-photon Rabi frequency, Δ is the total (red) detuning, and $C_6 > 0$ is the van der Waals coefficient. The
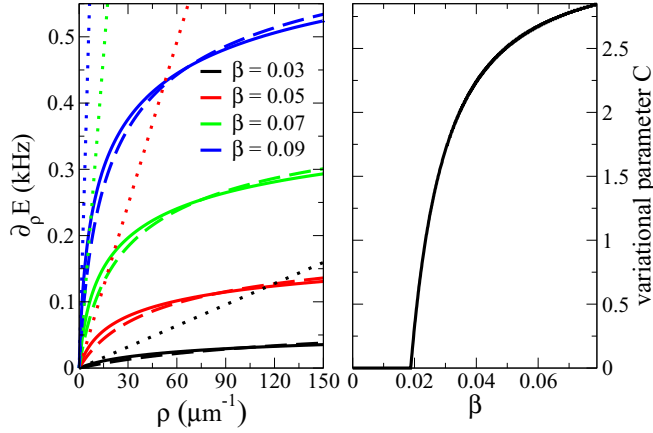
FIG. 1. Left panel: Characteristic behavior of the Rydberg-dressed interaction in 1D, as a function of BEC linear density, for realistic experimental conditions, using the $35S$ Rydberg state of ^{87}Rb. The energy functional $\partial_\rho E[\rho]$ is plotted for different dressing Rabi frequencies, as parameterized by $\beta = \Omega/2|\Delta|$ for fixed detuning $\Delta/2\pi = -100$ kHz. Corresponding critical densities ρ_B are (curves from bottom to top) 177 μm^{-1}, 64 μm^{-1}, 33 μm^{-1}, and 20 μm^{-1}. Dashed lines correspond to the variational ansatz F, Eq. (3), and dotted lines correspond to a linear increase with density as in the two-body limit. Right panel: Variational parameter C for the energy functional ansatz F. Vanishing C for $\beta < 0.018$ corresponds to the two-body limit, Eq. (1), while $\beta > 0.018$ corresponds to the saturation effect, Eq. (5).

resulting interaction potential between dressed atoms has the form $W(r) = \beta^4 \frac{C_6}{R_B^6 + r^6}$ [12]. In practice, the blockade radius R_B is in the micrometer range.

While the Rydberg-dressed interaction can be strong because of the high value of C_6, for larger densities (typical for a BEC) it saturates around the characteristic density $\rho_B = 1/\beta^2 V_B$, where there is one excited Rydberg atom per Rydberg blockade volume V_B. This leads to an overall offset of the chemical potential of the BEC, but only to a small modification of the shape compared to no dressing. Only for low relative density, $\rho < \rho_B$, is there a significant alteration of the BEC shape due to dressing. In 3D, as considered in Ref. [31], one has $V_B = \frac{4}{3}\pi R_B^3$ and for typical parameters ρ_B is lower than that of typical densities of 3D BECs. In contrast, in the 1D case we consider here, one has a 1D blockade volume of $V_B = 2R_B$, leading to a different scaling of ρ_B. We find that for practical experimental conditions the entire 1D BEC can have a density below ρ_B.

We now give a quantitative description of the effects of the Rydberg dressing on a (effectively) 1D BEC. We assume a cigar-shaped BEC, in a trap with a radial trapping frequency, $\omega_\perp$, much larger than the axial trapping frequency ω_0 and a chemical potential of $\mu < \hbar\omega_\perp$. We start from the generalized Gross-Pitaevskii (GP) equation $i\hbar \frac{\partial \psi(x)}{\partial t} = [-\frac{\hbar^2 \partial_x^2}{2m} + g_0 N |\psi(x)|^2 + \frac{m\omega_0^2 x^2}{2} + V_{\mathrm{MF}}]\psi(x)$, where N is the particle number and $g_0 = 2a_s\hbar\omega_\perp$ is the 1D mean-field coupling parameter. In the mean-field regime, and assuming the radial size of the BEC is much smaller than R_B (and at sufficiently low densities where collective effects can be neglected), $V_{\mathrm{MF}} = N \int W(x - x')|\psi(x')|^2 dx'$, which is

treated in the same way as recently shown in Rydberg physics [10,15]. If we assume that the length of the 1D BEC is much larger than the Rydberg blockade radius R_B, so that the density is constant over this radius, we may approximate the V_{MF} term as $V_{\mathrm{MF}} \approx N|\psi(x)|^2 \int W(x')dx'$. Contrary to the bare van der Waals interaction, the combination of short-range saturation and a long-range $1/r^6$ tail of the two-body dressed interaction assures that the above integral is finite, and therefore gives a correction to the 1D mean-field coupling g_0 of

$$g_{\mathrm{eff}} = g_0 + \frac{2}{3}\pi \frac{C_6}{R_B^5}\beta^4 = g_0 + \frac{\pi}{12}\frac{\hbar\Omega^4}{|\Delta|^3}R_B, \qquad (1)$$

and corresponds to a linear increase of $\partial_\rho E$ with density in Fig. 1. Note that when these conditions are applied to a 3D BEC, we similarly find $g_{\mathrm{eff}}^{\mathrm{3D}} = g_0^{\mathrm{3D}} + \frac{2}{3}\pi^2 \frac{C_6}{R_B^3}\beta^4 = g_0^{\mathrm{3D}} + \frac{\pi^2}{12}\frac{\hbar\Omega^4}{|\Delta|^3}R_B^3$, which has already been derived in Refs. [12,30,31].

Next, to allow for higher linear densities where collective effects can play a role, we adapt the treatment of Ref. [12] to 1D, again using the assumption that the radial size of the BEC is much smaller than R_B. In this way, we obtain an energy density for the internal degrees of freedom ϵ_{var} at linear density ρ,

$$\epsilon_{\mathrm{var}}(\theta,\xi) = \frac{\hbar\Delta\rho}{2}\cos 2\theta - \frac{\hbar\Omega\rho}{2}\sin 2\theta + \frac{\lambda}{2}\sin^4\theta \frac{C_6\rho^2}{\xi^5}, \quad (2)$$

having as variational parameters the Rydberg mixing angle θ and the correlation length ξ. Note that in 1D the last term scales as ξ^{-5}, compared to ξ^{-3} in 3D. The correlation length ξ is constrained to the blockade radius R_B for low densities and to the average distance between Rydberg atoms, $1/f\rho$, for higher densities; $\xi \approx \min(R_B, 1/f\rho)$, with $f = \sin^2\theta$ the Rydberg excitation fraction. In this approach, minimizing the energy density with respect to θ yields the energy functional $E[\rho]$, and the derivative $\partial_\rho E[\rho]$ (see solid lines in Fig. 1) is inserted as V_{MF} into the generalized GP equation. In the low-density limit of Eq. (2), one has $\xi = R_B$ and θ approaches β; comparing the result to the Rydberg part of the two-body limit Eq. (1) allows us to determine the value $\lambda = 2\pi/3$ in Eq. (2).

As a specific example, we consider dressing the ^{87}Rb ground state with the $n = 35S$ Rydberg state (which has $C_6/\hbar = 2\pi \times 0.1891$ GHz μm^6 [37]) and the detuning $\Delta = -2\pi \times 100$ kHz, leading to the blockade radius $R_B = 3.13 \mu$m. (Note that for $n < 50$ Rydberg dressing will not be affected by molecular dimer excitations, as the splitting between the dimer and the atomic excitation line is always greater than the typical linewidth of <1MHz [38]). The resulting energy functional is shown in Fig. 1 for various Rabi frequencies parametrized by β and as a function of the linear density ρ. For the parameters and densities in Fig. 1 we find $R_B < 1/f\rho$, and thus we may take $\xi = R_B$ throughout. It is worth emphasizing here that the saturation in the energy functional as the density increases is much less severe in 1D when compared to 3D and that the densities of 1D BECs in Fig. 1 are in the range that is typical for those achieved on atom chips [34–36].

A useful approximate description can be obtained as follows: the energy functional $E[\rho]$ is qualitatively described

by the anzatz

$$F[\rho] = \epsilon_0 - \epsilon_0 \left(1 + \frac{2}{3}\pi C \frac{\rho}{\rho_B}\right)^{-1/C}, \qquad (3)$$

which fulfills the two limiting cases: (i) it saturates for $\rho \gg \rho_B$ at a constant value of $\epsilon_0 = \hbar|\Delta|\beta^2$ [12]; (ii) it is linear with density for small densities, $F \approx \pi/12\hbar\Omega^4/|\Delta|^3 R_B\rho$ [see Eq. (1)]. The free parameter C is numerically obtained by minimizing the root mean square of the difference between F and $\partial_\rho E[\rho]$; these results are also shown in Fig. 1 as dashed lines. The linearization of Eq. (3) around the trap center allows us to extract the effective mean-field coupling constant g_{eff}. Because the Rydberg dressing will only have a small effect on the Thomas-Fermi profile, as is shown in the following paragraphs, we are able to express the dressing effect as an effective change of the trapping frequency. This is done by equating all the different potential energy terms in the GP equation:

$$g_0\rho + m\omega_0^2 x^2/2 + F[\rho] \approx g_0\rho + m\omega_{\text{eff}}^2 x^2/2$$
$$= g_{\text{eff}}\rho + m\omega_0^2 x^2/2, \qquad (4)$$

with ρ being the undressed Thomas-Fermi profile. After linearization of F around the trap center, we find the effective mean-field coupling constant including the saturation effects of dressing to be

$$g_{\text{eff}} = g_0 + \frac{\pi}{12}\frac{\hbar\Omega^4}{|\Delta|^3}R_B\left(1 + \frac{\pi}{3}C\frac{\rho_0}{\rho_B}\right)^{-1/C-1}, \qquad (5)$$

where ρ_0 is the BEC peak density and C is a variational parameter for Eq. (3). One can observe that the two-body limit is obtained for vanishing densities, as well as for $\beta < 0.018$ (see Fig. 1).

In order to further quantify the effects of Rydberg dressing on a 1D BEC, we now consider a more specific scenario. We assume a BEC of $N = 200, 1000, 2000$ ^{87}Rb atoms with an s-wave scattering length of $a_s = 99a_0$ (where a_0 is the Bohr radius) confined in a cylindrical harmonic trap with radial frequency $\omega_\perp = 2\pi\times 3000$ Hz and axial frequency $\omega_0 = 2\pi\times 30$ Hz. These parameters correspond to the mean-field coupling strength $g_0 = 2.08\times 10^{-38}$ Jm $= 0.53 E_0 l_0$, with $E_0 = \hbar\omega_0$, $l_0 = \sqrt{\hbar/m\omega_0} = 1.97$ μm, and $t_0 = \omega_0^{-1} = 5.3$ ms as energy, length, and time units, respectively. In the absence of dressing, the corresponding BEC half-length along the axial direction and the peak density are 10.6 μm and 28 μm^{-1} for $N = 200$, 18.2 μm and 81 μm^{-1} for $N = 1000$, and 23 μm and 128 μm^{-1} for $N = 2000$.

The effects of the Rydberg dressing can now be characterized as follows. For different particle numbers N and dressing parameters β (keeping $\Delta = -2\pi\times 100$ kHz fixed) we first calculate the ground state ψ_0 of the generalized GP equation, using $\partial_\rho E$ obtained from Eq. (2). Next, we calculate the time evolution of this initial wave packet upon a sudden switch-off of the Rydberg dressing and numerically calculate the relative change of the BEC size defined as $\kappa(t) = R(t)/R_0$, where R_0 is the initial dressed BEC half-length in the axial direction and $R(t)$ is the half-length in the axial direction obtained from fitting the parabola to the undressed cloud at time t.

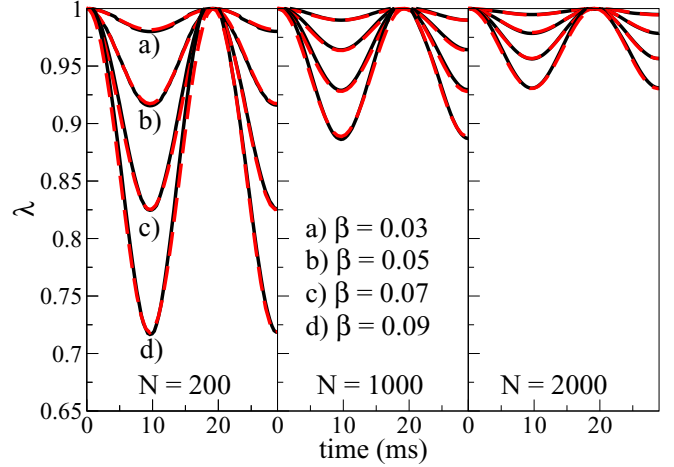This nonadiabatic switch-off of the dressing results in the excitation of a BEC breathing mode. The dynamics of a BEC

FIG. 2. Relative change of the BEC size after sudden switch-off of the dressing lasers (κ) for different BEC particle numbers and different dressing parameters. Red dashed lines correspond to the self-similar density evolution (λ).

can be described by the collective motion of atoms with the time-dependent density $\rho(x,t) \propto \rho_0[x/\lambda(t)]/\lambda(t)$, where $\rho_0(x)$ is the initial BEC density and the scaling parameter $\lambda(t)$ obeys $\frac{d^2\lambda}{dt^2} = \frac{\omega_{\text{eff}}^2}{\lambda^3} - \omega_0^2\lambda$ [39]. A solution of this equation is periodic, with an amplitude parametrized by ω_{eff} and the frequency $\omega_b \simeq \sqrt{3}\omega_0$. For fixed N, n, and β we calculate $\kappa(t)$, which we then use to find ω_{eff} by minimizing the root mean square of the difference between $\lambda(t)$ and $\kappa(t)$. Figure 2 presents κ (black solid lines) and λ (red dashed lines) for fixed numbers of atoms $N = 200, 1000$, and 2000 and fixed dressing parameters $\beta = 0.03, 0.05, 0.07$, and 0.09, with corresponding critical densities ρ_B equal to 177, 64, 33, and 20 μm^{-1}, respectively. Knowing ω_{eff} we can extract the effective density-dependent change of the mean-field interaction strength $g_{\text{eff}}/g_0 = (\omega_{\text{eff}}/\omega_0)^{-2}$. Figure 3 presents the change of the effective trapping frequency and of the
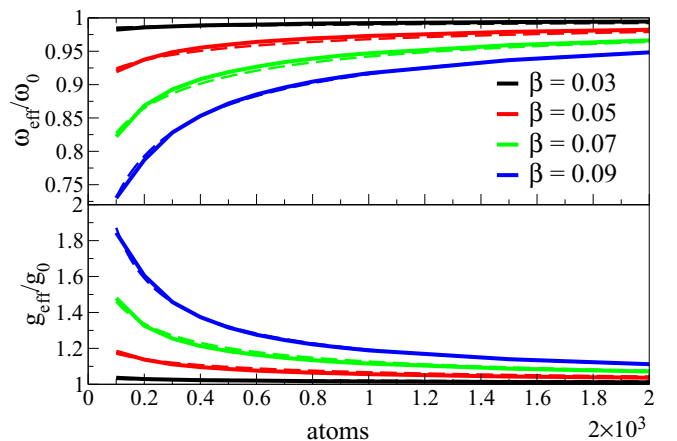

FIG. 3. Relative change of the effective trapping frequency ω_{eff} (top panel) and relative change of the mean-field coupling g_{eff} (bottom panel) for different atom numbers N for the fixed dressing parameter (curves from top to bottom: $\beta = 0.03, 0.05, 0.07$, and 0.09). Dashed lines correspond to Eq. (5).

effective mean-field interaction strength as a function of the particle number N, for the fixed dressing parameter β, which agrees very well with the analytical expression of Eq. (5).

An important consideration is the decay associated with the Rydberg dressing, including the effects of radiative decay of the intermediate state in the two-photon coupling scheme. In practice the atomic system is a three-level system with an atomic ground state $|g\rangle$ coupled to a Rydberg S-state $|r\rangle$ via an intermediate state $|e\rangle$. The Rabi frequency and detuning for the transition from $|g\rangle$ to $|e\rangle$ are Ω_1 and Δ_1, while similarly for the transition from the intermediate state $|e\rangle$ to the Rydberg state $|r\rangle$ they are denoted as Ω_2 and Δ_2. The intermediate level $|e\rangle = |5P_{3/2}\rangle$ is far detuned, i.e., $|\Delta_1|, |\Delta_2| \gg \Omega_1, \Omega_2, \Gamma_{5P_{3/2}}$ and can be adiabatically eliminated. This effectively reduces the three-level system to a two-level system with two-photon Rabi frequency $\Omega = \Omega_1\Omega_2/2|\Delta_1|$ and total detuning $\Delta = \Delta_1 + \Delta_2$, with $|\Delta| \ll |\Delta_1|, |\Delta_2|$.

As an example, we can take the red (780-nm wavelength) laser parameters as having a waist of $r_{\text{red}} = 500$ μm with a power of $P_{\text{red}} = 10$ μW and the blue (480-nm wavelength) laser parameters as having a waist of $r_{\text{blue}} = 90$ μm with a maximum power of $P_{\text{blue}} = 50$ mW with a fixed intermediate state detuning of $\Delta_1 = 2\pi \times 1.5$ GHz. Keeping the total detuning $\Delta = -2\pi \times 100$ kHz constant as before, we change the dressing parameter β via the Rabi frequency Ω_2. We calculate the lifetime of the Rydberg-dressed state by considering a weak admixture to the intermediate state $|5P_{3/2}\rangle$ with the decay rate $\Gamma_{5P_{3/2}}$ and an admixture of the Rydberg state $|r\rangle = |nS\rangle$ with the decay rate Γ_{nS}, which results in an effective decay rate smaller than $\Gamma_{\text{eff}} = \beta^2\Gamma_{nS} + (\Omega_1/2\Delta_1)^2\Gamma_{5P_{3/2}}$. (Note that the effective decay rate is smaller when collective effects play a role because in that case one should replace β^2 with f and $f < \beta^2$.) The lifetime Γ_{nS}^{-1} for the $n = 35S$ ^{87}Rb Rydberg state is 25.2 μs at temperature $T = 300$ K [40]. The intermediate state decay rate is $\Gamma_{5P_{3/2}} = 2\pi \times 6.1$ MHz, and $\Omega_1/2\Delta_1 = 18 \times 10^{-4}$. The corresponding minimum lifetimes for $\beta = 0.03, 0.05, 0.07,$ and 0.09 are then 6.3, 4.5, 3.1, and 2.2 ms, respectively. From these results, it is clear that it is realistic to observe Rydberg dressing in an experiment: for instance, for the parameters $N = 1000$ and $\beta = 0.07$, the resulting change in BEC size during the breathing is about 8%.

It should be possible to reach the dressed ground state by turning on the dressing lasers during the very final stages of evaporative cooling. An alternative approach is to consider adiabatic turn-on and rapid switch-off of the dressing; this is beyond the scope of the present paper. An advantage of the above scheme is that the resulting breathing occurs in the undressed BEC, so that the limited lifetime of the dressed state is not an issue during the breathing.

The Rydberg-mediated control over the interactions we have discussed here offers an important alternative to previously considered schemes. For instance, Feshbach resonances allow for time-dependent nonlinear dynamics as they can be utilized for a periodic modification of the mean-field coupling. This was proposed by Saito and Ueda [41], who considered a sinusoidal time-dependent modulation of the coupling constant, and by Kevrekidis *et al.* [42], who considered a block type of periodic modulation of the mean-field coupling constant. An intriguing opportunity offered by the dressing is that by spatially modulating the dressing lasers (e.g., in a standing wave) it would be possible to create a *spatial* modulation of the interaction strength, as well as a temporal modulation, which can be rapidly switched.

[1] M. D. Lukin, M. Fleischhauer, R. Côté, L. M. Duan, D. Jaksch, J. I. Cirac, and P. Zoller, Phys. Rev. Lett. **87**, 037901 (2001).

[2] R. Heidemann, U. Raitzsch, V. Bendkowsky, B. Butscher, R. Löw, L. Santos, and T. Pfau, Phys. Rev. Lett. **99**, 163601 (2007).

[3] E. Urban, T. A. Johnson, T. Henage, L. Isenhower, D. D. Yavuz, T. G. Walker, and M. Saffman, Nat. Phys. **5**, 110 (2009).

[4] A. Gaëtan, Y. Miroshnychenko, T. Wilk, A. Chotia, M. Viteau, D. Comparat, P. Pillet, A. Browaeys, and P. Grangier, Nat. Phys. **5** 115 (2009).

[5] H. Weimer, R. Löw, T. Pfau, and H. P. Büchler, Phys. Rev. Lett. **101**, 250601 (2008).

[6] T. Pohl, E. Demler, and M. D. Lukin, Phys. Rev. Lett. **104**, 043002 (2010).

[7] R. M. W. van Bijnen, S. Smit, K. A. H. van Leeuwen, E. J. D. Vredenbregt, and S. J. J. M. F. Kokkelmans, J. Phys. B: At. Mol. Opt. Phys. **44**, 184008 (2011).

[8] J. Schachenmayer, I. Lesanovsky, A. Micheli, and A. J. Daley, New J. Phys. **12**, 103044 (2010).

[9] J. D. Pritchard, D. Maxwell, A. Gauguet, K. J. Weatherill, M. P. A. Jones, and C. S. Adams, Phys. Rev. Lett. **105**, 193603 (2010).

[10] N. Henkel, R. Nath, and T. Pohl, Phys. Rev. Lett. **104**, 195302 (2010).

[11] J. E. Johnson and S. L. Rolston, Phys. Rev. A **82**, 033412 (2010).

[12] J. Honer, H. Weimer, T. Pfau, and H. P. Büchler, Phys. Rev. Lett. **105**, 160404 (2010).

[13] D. Jaksch, J. I. Cirac, P. Zoller, S. L. Rolston, R. Côté, and M. D. Lukin, Phys. Rev. Lett. **85**, 2208 (2000).

[14] H. Weimer, M. Müller, I. Lesanovsky, P. Zoller, and H. P. Büchler, Nat. Phys. **6**, 382 (2010).

[15] M. Mukherjee, J. Millen, R. Nath, M. P. A. Jones, and T. Pohl, J. Phys. B: At. Mol. Opt. Phys. **44**, 184010 (2011).

[16] T. Keating, K. Goyal, Y-Y. Jau, G. W. Biedermann, A. J. Landahl, and I. H. Deutsch, Phys. Rev. A **87**, 052314 (2013).

[17] T. Macrì and T. Pohl, Phys. Rev. A **89**, 011402 (2014).

[18] A. W. Glaetzle, M. Dalmonte, R. Nath, C. Gross, I. Bloch, and P. Zoller, Phys. Rev. Lett. **114**, 173002 (2015).

[19] R. M. W. van Bijnen and T. Pohl, Phys. Rev. Lett. **114**, 243002 (2015).

[20] G. Pupillo, A. Micheli, M. Boninsegni, I. Lesanovsky, and P. Zoller, Phys. Rev. Lett. **104**, 223002 (2010).

[21] M. Boninsegni, J. Low Temp. Phys. **168**, 137 (2012).

[22] N. Henkel, F. Cinti, P. Jain, G. Pupillo, and T. Pohl, Phys. Rev. Lett. **108**, 265301 (2012).

[23] F. Grusdt and M. Fleischhauer, Phys. Rev. A **87**, 043628 (2013).

[24] P. Mason, C. Josserand, and S. Rica, Phys. Rev. Lett. **109**, 045301 (2012).

[25] M. Kunimi and Y. Kato, Phys. Rev. B **86**, 060510 (2012).

[26] T. Macrí, F. Maucher, F. Cinti, and T. Pohl, Phys. Rev. A **87**, 061602 (2013).

[27] Y.-Y. Jau, A. M. Hankin, T. Keating, I. H. Deutsch, and G. W. Biedermann, Nat. Phys. **12**, 71 (2016).

[28] J. Zeiher, R. van Bijnen, P. Schauss, S. Hild, J-Y. Choi, T. Pohl, I. Bloch, and C. Gross, Nat. Phys. **12**, 1095 (2016).

[29] C. Gaul, B. J. DeSalvo, J. A. Aman, F. B. Dunning, T. C. Killian, and T. Pohl, Phys. Rev. Lett. **116**, 243001 (2016)

[30] F. Maucher, N. Henkel, M. Saffman, W. Krolikowski, S. Skupin, and T. Pohl, Phys. Rev. Lett. **106**, 170401 (2011).

[31] J. B. Balewski, A. T. Krupp, A. Gaj, S. Hofferberth, R. Löw, and T. Pfau, New J. Phys. **16**, 063012 (2014).

[32] W. Li, L. Hamadeh, and I. Lesanovsky, Phys. Rev. A **85**, 053615 (2012).

[33] R. Mukherjee, C. Ates, W. Li, and S. Wüster, Phys. Rev. Lett. **115**, 040401 (2015).

[34] T. Schumm, S. Hofferberth, L. M. Andersson, S. Wildermuth, S. Groth, I. Bar-Joseph, J. Schmiedmayer, and P. Krüger, Nat. Phys. **1**, 57 (2005).

[35] J. Estève, J.-B. Trebbia, T. Schumm, A. Aspect, C. I. Westbrook, and I. Bouchoule, Phys. Rev. Lett. **96**, 130403 (2006).

[36] A. H. van Amerongen, J. J. P. van Es, P. Wicke, K. V. Kheruntsyan, and N. J. van Druten, Phys. Rev. Lett. **100**, 090402 (2008).

[37] K. Singer, J. Stanojevic, M. Weidemüller, and R. Côté, J. Phys. B: At. Mol. Opt. Phys. **38**, 295 (2005).

[38] A. Gaj *et al.*, Nat. Commun. **5**, 4546 (2014).

[39] Y. Castin and R. Dum, Phys. Rev. Lett. **77**, 5315 (1996).

[40] I. I. Beterov, I. I. Ryabtsev, D. B. Tretyakov, and V. M. Entin, Phys. Rev. A **79**, 052504 (2009).

[41] H. Saito and M. Ueda, Phys. Rev. Lett. **90**, 040403 (2003).

[42] P. G. Kevrekidis, G. Theocharis, D. J. Frantzeskakis, and B. A. Malomed, Phys. Rev. Lett. **90**, 230401 (2003).